Graphical Abstract

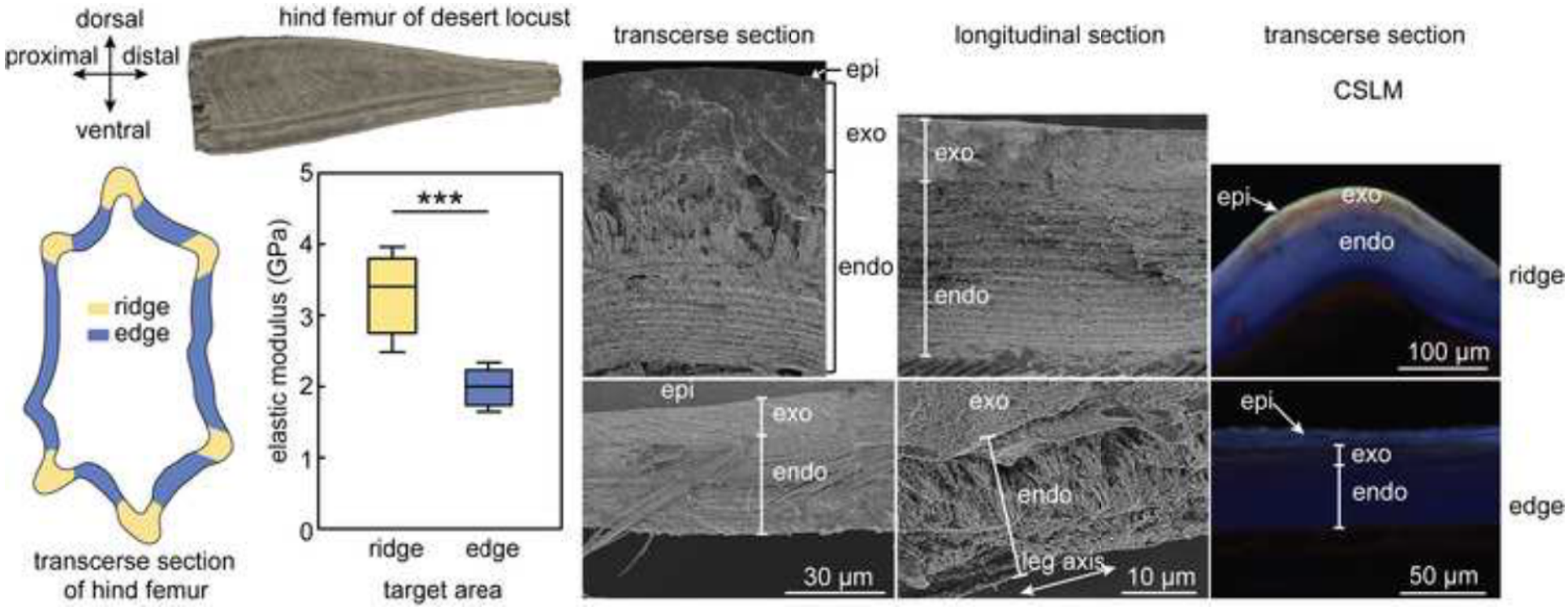

Biomechanical strategies to reach a compromise between stiffness and flexibility in hind femora of desert locusts

Chuchu Li*, Stanislav N. Gorb, Hamed Rajabi

Functional Morphology and Biomechanics, Institute of Zoology, Kiel University, Kiel, Germany

* Corresponding author: cli@zoologie.uni-kiel.de

Abstract: Insect cuticle can reach a wide range of material properties, which is thought to be the result of adaptations to applied mechanical stresses. Biomechanical mechanisms behind these property variations remain largely unknown. To fill this gap, here we performed a comprehensive study by simultaneous investigation of the microstructure, sclerotization and the elasticity modulus of the specialized cuticle of the femora of desert locusts. We hypothesized that, considering their different roles in jumping, the femora of fore-, mid- and hind legs should be equipped with cuticles that have different mechanical properties. Surprisingly, our results showed that the hind femur, which typically bears higher stresses, has a lower elasticity modulus than the fore and mid femora in the longitudinal direction. This is likely due to the lower sclerotization and different microstructure of the hind femur cuticle. This allows for some deformability in the femur wall due to mechanical stresses caused by jumping and reduces the risk of mechanical failure. In contrast to both other femora, the hind femur is also equipped with a set of sclerotized ridges that are likely to provide it with the required stiffness to withstand loads. This paper is one of only a few comprehensive studies on insect cuticle, which advances the current understanding of the relationship between the structure, material property and function in this complex biological composite.

Keywords: biomechanics, nanoindentation, microstructure, functional adaptation, muscle, insect, cuticle.

1. Introduction

Insect cuticle is a complex biological composite. It consists of chitin fibers that are embedded in a protein matrix (Locke, 1974). Cuticle is often made of three main layers of epicuticle, exocuticle and endocuticle, which differ in the microstructure, sclerotization and material properties (Richards, 1958; Neville, 1975; Andersen, 1979; Michels et al., 2016). Being a physical interface between environment and insect internal organs, cuticle serves a few key functions: (i) protection against mechanical impacts, (ii) providing a robust attachment site for muscles and sensory organs, and (iii) facilitating the ion and water balance of insect body (Locke, 1974; Neville, 1975).

Cuticles of different body parts have undergone biomechanical adaptations to their respective functions. An example is the prothorax cuticle of beetles, such as *Copris ochu* and *Holotrichia sichotana*, which has the function of support and protection. It has reached an elasticity modulus that is about 2~4 times higher than in other tested body parts (Sun et al., 2008). Such local adaptations of cuticle properties also exist in other body parts, such as legs. In locusts, for example, hind legs, in comparison to other legs, play a key role in generating jump forces. Hence, hind tibiae are equipped with a cuticle that is about two times stiffer than that of fore and mid tibiae (Parle et al., 2016; Li et al., 2020). Functional adaptations can also be found within certain other leg parts, such as single setae of adhesive pads of the ladybird beetle *Coccinella septempunctata* (Peisker et al., 2013). The elasticity modulus significantly varies from 6.8 GPa at the base to 1.2 MPa at the tip of the setae. This dramatic gradient in the stiffness was interpreted as a functional adaptation to enhance the adjustment of the insect attachment system to rough substrates.

Although the existing data support the presence of specialized adaptations of insect cuticle to applied mechanical stresses, mechanisms through which such adaptations are achieved remain largely unknown. This is mainly due to the lack of a clear understanding of the relationship between the microstructure, sclerotization, material properties and function in insect cuticle. There are only a few studies in the literature that have investigated the link between the mentioned parameters (Goodwyn et al., 2006; Müller et al., 2008; Peisker et al., 2013; Scholz et al., 2008; Matsumura et al., 2017; Wan et al., 2016; Wang et al., 2018b; Li et al., 2020). To fill this gap in the literature, here we performed a comprehensive study on a

specialized leg segment of the locust, femur. The femura were chosen, because, unlike any other cuticles selected by previous studies, they have to support large amount of muscles. Our aim is to deepen the existing understanding of the relationship between the structure, material property and function in insect cuticle. We employ here micro-computed tomography (micro-CT), scanning electron microscopy (SEM), confocal laser scanning microscopy (CLSM) and nanoindentation to simultaneously study the microstructure, the sclerotization level and the elasticity modulus of the femoral cuticle. We have chosen nanoindentation, because it is perhaps one of the most suitable methods for our purpose of measuring the elastic modulus of the anisotropic cuticle. Considering different forces that femora of different legs withstand during locomotion, we hypothesize that they have utilized different biomechanical strategies to achieve desired mechanical properties. In particular, we expect that the elasticity modulus of the hind femur, if not equal, is higher than that of the fore and mid femora. Our results help to shed light on the biomechanics of the complex composite material of insect cuticle.

2. Materials and Methods

2.1. Ethics

All procedures in this study comply with ethical guidelines at Kiel University.

2.2. Specimens

The locusts *Schistocerca gregaria* were bought from pet shops in Kiel, Germany. They were kept under a natural day/night cycle in an environment with controlled temperature (25 °C-30 °C) and humidity (30%-40%). They were fed with fresh grass and vegetables. We experimented only with adult individuals that were at ≥ 21 days post molt.

2.3. Three-dimensional visualization using Micro-CT

Fore, mid and hind femora were dehydrated in an ascending ethanol series, and critical-point dried in a Leica CPD300 critical-point drier (Leica Microsystems GmbH, Wetzlar, Germany). The dried specimens were then scanned using a SkyScan 1172 tabletop micro-CT scanner (Bruker micro-CT, Kontich, Belgium) at a source voltage of 40 kV, a current of 250 μA and with a resolution of 6.15 μm. Segmentation and visualization of the data were done with Amira v.5.4.3 (FEI Visualization Sciences Group, Bordeaux, France) and

ImageJ v.1.5i (National Institutes of Health, Bethesda, MD). Three femora from three different individuals were scanned for each leg.

2.4. Measurement of mechanical properties by nanoindentation

Prior to mechanical testing, adult locusts were euthanized with CO_2. Fresh fore, mid, and hind legs were removed. Pieces of ~2.0 × 2.0 × 1.0 mm^3 size were separated from the mid parts of femora using a razor blade. They were fixed on a specimen holder, within 2 min after the dissection, using super glue (5925 Ergo, Kisling AG, Wetzikon, Switzerland). The specimen surfaces were polished by sandpaper with a grain diameter of 0.3 μm (ITW Test & Measurement GmbH, Esslingen, Germany). Wet cotton, covered with parafilm (BEMIS Packaging Deutschland GmbH, Rheinbach, Germany), was used to surround the specimens, in order to minimise desiccation during measurements (Li et al., 2020). The measured elastic moduli of locust cuticle, by this method, have shown good consistency against time (Fig. S1).

The specimens were indented using a SA2 Nanoindenter (MTS Nano Instruments, Oak Ridge, Tenn., USA) equipped with a Berkovich diamond tip. The elasticity modulus of the specimens was measured using continuous stiffness measurement (CSM) technique. Nanoindentations were performed on samples oriented in three different directions, to allow estimations of their elasticity moduli in: (i) the longitudinal direction (i.e., along the length of the femur), (ii) the circumferential direction (i.e., along the circumference of the femur), and (iii) the radial direction (i.e., the direction pointing to the endocuticle from the epicuticle) (Fig. 1b). Nanoindentations were performed on ten sites on each sample. The distance between adjacent indentation sites on the surface of each specimen was set to be > 30 μm, to avoid the interference between consecutive measurements. The maximum indentation depth was set as 2 μm. The measurements for these ten sites were later averaged for the statistical tests. In total, 45 samples taken from 45 individuals were tested.

2.5. Visualization of cuticle sclerotization by confocal laser scanning microscopy (CLSM)

Active adult locusts were euthanized by deep freezing at -70° for ~3 min. The legs were then cut off by a scalpel. The legs were fixed on a glass plate using double side tape. Transverse sections of fore, mid and hind femur with a thickness ~300 μm were made using a sharp razor blade. The specimens were washed with 75% ethanol and then immersed in glycerin (≥99.5%, Carl Roth GmbH & Co. KG, Karlsruhe, Germany). After fixing the

specimens in glycerin between a glass slide and a cover slip (Carl Roth GmbH & Co. KG, Karlsruhe, Germany) for ~2 h, we visualized them with the CLSM (Zeiss LSM 700, Carl Zeiss Microscopy, Jena, Germany). The CLSM was equipped with four lasers (laser lines: 405 nm, 488 nm, 555 nm, 639 nm) to excite the samples subsequently. Four emission filters transmitting 420-480 nm, ≥ 490 nm, ≥ 560 nm and ≥ 640 nm were used to visualize the autofluorescence of the femoral cuticle. To account for the thickness of specimens, we used Z-stack imaging and took multiple images at different focal planes through the entire thickness of the specimens. We then created maximum intensity projections by means of the Zeiss Efficient Navigation (ZEN) software (Carl Zeiss MicroImaging GmbH), based on the collected image stacks. In total, three transverse sections of each leg femur from three individuals were scanned.

The obtained RGB CLSM images were used to represent the sclerotization level of insect cuticle (Michels and Gorb, 2012). Non-sclerotized cuticle autofluoresces in blue; less-sclerotized cuticle autofluoresces in green and yellow (overlay of green and a little bit red); highly-slcerotized cuticle is dominated by the red autofluorescence. The obtained CLSM images were split into three primary channels (i.e. R, G, B), and transformed into gray scale images using ImageJ v.1.5i (National Institutes of Health, Bethesda, MD). The sclerotization level of the cuticle was then measured based on the intensity of each primary color (Eshghi et al., 2018). We used the intensity of each primary color as a measure of the proportion of the material emitting that primary in the CLSM image. For example, the stronger intensity of the red color, in comparison to green and blue colors in a cuticle specimen suggests the higher proportion of the sclerotized cuticle in comparison to the less- and non-sclerotized cuticle.

2.6. Microstructural characterization of the cuticle with scanning electron microscopy (SEM)

The legs were cut from freshly killed locusts. Small cracks were made on the femur surface using a scalpel. The fractured femora were dehydrated in an ascending ethanol series (70%, 80%, 90% ethanol once and 100% ethanol three times, each step - 20 min), and critical-point dried in a Leica CPD300 critical-point drier (Leica Microsystems GmbH, Wetzlar, Germany). The dried femora were broken at the initiated cracks and then mounted on SEM stubs with carbon Leit-tabs (Plano GmbH, Wetzlar, Germany). After sputter-coating with gold-palladium (6-10 nm thickness) using a Leica EM sputter coater (SCD 500

High-Vacuum, Leica Microsystems GmbH, Wetzlar, Germany), they were examined in a scanning electron microscope Hitachi S-4800 (Hitachi High-Tech., Tokyo, Japan). Eighteen transverse sections and eighteen longitudinal sections of each femur from six individuals were examined in total. This included samples taken from the femur basal part (close to the body), middle and distal part (close to the tibia).

2.7. Statistical analysis

All the statistical tests in the present study are two-tailed and performed in Sigmaplot v.12.5 (Systat Software GmbH, Erkrath, Germany). Assumptions of normality and homogeneity of variances were tested by Shapiro-Wilk test before further analysis. The elasticity moduli obtained from nanoindentations were compared between the fore, mid and hind femora in each direction, and between the different directions for each femur by Holm-Sidak two-way ANOVA test. The area proportion of non-, less- and highly-sclerotization cuticle were compared between different femora by Holm-Sidak one-way ANOVA. All values shown in the manuscript are mean ± s.d.

3. Results

3.1. Comparison of the elasticity moduli of femora in different directions

We measured the elasticity moduli of each femur in three orthogonal directions, i.e. the longitudinal, circumferential and radial directions (Fig. 1b). The elasticity moduli of the fore, mid and hind femora were equal to 6 ± 1 GPa, 6.0 ± 0.5 GPa and 2.0 ± 0.3 GPa, in the longitudinal direction, 1.5 ± 0.4 GPa, 2.1 ± 0.5 GPa and 3.8 ± 0.7 GPa, in the circumferential direction, and 2.5 ± 0.4 GPa, 2.7 ± 0.8 GPa and 2.3 ± 0.7 GPa, in the radial direction, respectively (Fig. 2).

Statistical analyses showed that the elasticity moduli were significantly different both between the legs and between the measurement directions ($P<0.001$, two-way ANOVA). In the fore and mid femora, significant differences in the elasticity moduli were found between the longitudinal direction (n = 5) and circumferential (n = 5) /radial direction (n = 5) ($P<0.001$, Holm-Sidak two-way ANOVA). In the hind femur, significant differences were found between the circumferential direction (n = 5) and the longitudinal (n = 5)/radial direction (n = 5) ($P<0.001$/$P = 0.003$, Holm-Sidak two-way ANOVA). Comparison of the elasticity moduli

between the femora showed significant differences between the fore/mid femur and hind femur in the longitudinal and circumferential directions ($P<0.001$, Holm-Sidak two-way ANOVA). The results of the statistical analyses are summarized in Table 1 using all pairwise multiple comparison procedures (Holm-Sidak method). .

Table 1. Comparison of the elasticity moduli of femora of different legs in different directions. Significant differences are given for the elasticity moduli of the fore (n = 15), mid (n = 15), and hind femora (n = 15) in each direction and between the elasticity moduli of the femora in the longitudinal, circumferential and radial directions. *: P<0.05, **: P<0.01, and ***: P<0.001. FL: fore femur in the longitudinal direction (n = 5), FC: fore femur in the circumferential direction (n = 5), FR: fore femur in the radial direction (n = 5), ML: mid femur in the longitudinal direction (n = 5), MC: mid femur in the circumferential direction (n = 5), MR: mid femur in the radial direction (n = 5), HL: hind femur in the longitudinal direction (n = 5), HC: hind femur in the circumferential direction (n = 5), HR: hind femur in the radial direction (n = 5).

	FL	FC	FR	ML	MC	MR	HL	HC	HR
FL		***	***	/	/	/	***	/	/
FC			*	/	/	/	/	***	/
FR				/	/	/	/	/	/
ML					***	***	***	/	/
MC						/	/	***	/
MR							/	/	/
HL								***	/
HC									**
HR									

3.2. Comparison of the sclerotization levels of the femoral cuticles

According to previous studies, the intensity of the blue, green and red autofluorescence in the CLSM image of a cuticular sample can be used as a measure of the relative amount the non-, less- and highly-sclerotized cuticle in the sample (Michels and Gorb, 2012; Eshghi et al., 2018; Rajabi et al., 2018; Li et al., 2020; Matsumura et al., 2020). We used the same approach here to estimate the proportion of the non-, less- and highly-sclerotized cuticle, as a fraction of the total femur transverse section area (Fig. 3). The area fraction of the non-sclerotized cuticle in the fore, mid and hind femora was 51 ± 4%, 51 ± 4% and 63 ± 4%, respectively. The area fraction of the less-sclerotized cuticle in fore, mid and hind femora was 37 ± 4%, 36 ± 3% and

26 ± 4%, respectively. The area fraction of the highly-sclerotization cuticle in fore, mid and hind femora was 10 ± 4%, 10 ± 2% and 13 ± 3%, respectively. Significant differences were found in the area fraction of the non-sclerotization cuticle between the fore (n = 3)/mid femora (n = 3) and the hind femur (n = 3) ($P<0.001$, Holm-Sidak one-way ANOVA), and in the area fraction of less-sclerotized cuticle between the fore (n = 3)/mid femora (n = 3) and the hind femur (n = 3) ($P<0.001$, Holm-Sidak one-way ANOVA). No significant difference was found in the area fraction of the highly-sclerotized cuticle between the femora ($P = 0.252$, Holm-Sidak one-way ANOVA).

3.3. Comparison of the microstructures of the femora cuticle

We investigated the microstructure of the femoral cuticle in the transverse and longitudinal directions from SEM. The cuticle of the fore, mid and the edge of hind femora consisted of the typical layers of the epi-, exo- and endocuticle (Fig. 4). The outer epicuticle layer is unstructured and very thin with a thickness of 590 ± 90 nm, 630 ± 70 nm and 740 ± 70 nm in the fore, mid and the edge of hind femora, respectively. The exocuticle of the femora showed dense sublayers that seem to have a helicoidal architecture, similar to that reported by Neville (1975), with a thickness of 14 ± 2 μm, 13 ± 2 μm and 13 ± 1 μm in the fore, mid and the edge of hind femur, respectively. The endocuticle consisted of multiple distinguishable layers of seemingly alternating helicoidal and unidirectional layers, as that previously observed in locust tibiae (Li, et al., 2020). The fibers in the unidirectional layers of the fore femur (Fig. 4a,b) and the mid femur (Fig. 4c,d) are oriented along the femur length. In contrast, the layers in the edge of hind femur are oriented along the femur circumference (Fig. 4e,f). The thickness of the endocuticle in the fore, mid and the edge of hind femora is 68 ± 9 μm, 90 ± 20 μm, 35 ± 5 μm, respectively.

The structure of the hind femur is notably different from the fore and mid femora (Fig. 1a). The fore and mid femora have circular transverse sections, whereas the hind femur has a seemingly hexagonal transverse sectional shape. At each corner, the hind femur has a pronounced ridge (Fig. 5a). We measured the mechanical properties of the ridges and characterized their sclerotization level and microstructure. The elasticity modulus of the ridges, measured in the longitudinal direction, was 3.3 ± 0.6 GPa. This is significantly different from the elasticity modulus of the other parts of the hind femur, here called edges, in

the same direction, 2.0 ± 0.3 GPa (n = 5, t-test, P = 0.002) (Fig. 5b).

The CLSM images demonstrated a noticeably higher red autofluorescence and a lesser blue autofluorescence at the ridges, compared with the edges. This indicates that the ridges are more sclerotized than the edges. Our SEM images showed that the epi- and exocuticle of the ridges were similar to those of the fore femur, mid femur and that of the edges of the hind femur, in both thickness and presence of the microstructure (Fig. 5e). However, the endocuticle of the ridges was different. The thickness of the endocuticle of the ridges was 73 ± 8 μm, about two times thicker than that of the edges. Furthermore, the majority of the fibers in the upper part of the endocuticle of the ridges were oriented along the length of the femur (Fig. 5e).

4. Discussion

4.1. Anisotropy of the femur stiffness: the role of the cuticle architecture

Our results showed direction dependency of the elasticity modulus of the femoral cuticle. This anisotropy can be explained by the architecture of the endocuticle, which forms the major portion of the femoral cuticle. We have seen that the majority of the fibers in each femur are oriented in a particular direction (i.e. along the longitudinal direction in the fore and mid femora and in the circumferential direction in the hind femur) (Fig. 4). This is an important observation. First, because this suggests the strong role of the fiber orientation in the stiffness of the femoral cuticle. Second, because it explains why the fore and mid femora have their highest elasticity moduli in the longitudinal direction, whereas the hind femur cuticle is the stiffest in the circumferential direction.

The dependency of the elasticity modulus of the femoral cuticle on fiber orientation is an interesting finding that helps to better understand the mechanical behavior of insect cuticle and that of other arthropods. Arthropod cuticle has been typically classified into two groups of ‘solid’ and ‘compliant’ ones (Hepburn and Chandler, 1976). Whereas the former type, i.e. the solid cuticle, serves a protective function, the latter, i.e. the compliant cuticle, often occurs in arthrodial membranes allowing the relative motion of body parts (Vincent, 1981; Wang et al., 2019). In the typical solid cuticle, stiffness is dominated by a sclerotized protein matrix that stabilizes the cuticle. In contrast, the stiffness of the compliant cuticle is mainly determined by fibers and their orientation within a flexible matrix. This categorization, however,

represents two extreme cases; some cuticles fit into neither category. The studied femoral cuticle represents an 'intermediate' example: although, from a functional point view, it fits better to the category of solid cuticles, its stiffness is apparently influenced by fiber orientations, as observed in the typical compliant cuticles. Thus, we can conclude that this specialized cuticle has undergone adaptations to both functions of protection and locomotion.

We have also seen that cuticle microstructure contributes to the difference in elastic moduli of the ridges and the edges in the hind femur (Fig. 5). The endocuticle of the ridges contains many sublayers with fibers that are oriented along the longitudinal axis of the femur (Fig. 5e-g). When indented in this direction, therefore, the stiffness of the ridges is dominated by the elastic modulus of the fibers in their longitudinal direction. In contrast to the ridges, under the same loading scenario, the stiffness of the edges is influenced by the elasticity modulus of the fibers in their lateral direction (the fibers are orientated circumferentially). Considering that the fibers are stiffer along their length than any other direction, this explains why the ridges have a higher elastic modulus than the edges.

Why are the majority of the fibers in the hind femur oriented in a different direction than those in the fore and mid femora? We suggest that this may be an adaptation to forces applied to the hind femur during jumping. The jumping muscle, *the extensor tibialis*, occupies a large part of the hind femur and generates the force required for jumping. The attachment site of the muscle on the femur cuticle provides the necessary mechanical support for the muscle contraction (Caveney, 1969). This means that the femoral cuticle should be robust enough to resist jumping forces, which can reach several times the body weight of the insect (Heitler, 1977). Considering how the muscles are attached to the inner part of the femur (see Fig. 1 in Hoyle, 1955), during jumping, the femur cuticle experiences large lateral strains caused by the muscle contraction (Gabriel, 1985). These strains, however, are rather small in practice (Bennet-Clark, 1975). We expect this to be the result of the specific architecture of the hind femur cuticle, with circumferentially oriented fibers, which provide a greater lateral support in comparison to fibers that are oriented longitudinally, preventing the lateral collapse of the femur in jumping events.

4.2. Femur stiffness: Complementary and conflicting roles of the microstructure and sclerotization

Sclerotization is a process during which the cross-linking of protein molecules stabilizes cuticle. Previous studies have shown the presence of a direct relationship between the sclerotization and stiffness of insect cuticle (Hepburn and Joffe, 1974; Peisker et al., 2013; Schmitt et al., 2018; Wang et al., 2018b; 2019; Li et al., 2020). Here we have seen a similar relationship between the two characteristics: the lower elasticity modulus of the hind femur in the longitudinal direction in comparison with the fore and mid femora, is accompanied with a lesser area proportion of the less- and highly-sclerotized cuticle (Fig. 3).

However, our results show that the relationship between the sclerotization and stiffness may not always be as straightforward as expected. In general, multiple factors can influence the mechanical properties of insect cuticle (Hepburn and Chandler, 1976), among which both the microstructure and sclerotization play key roles in determining cuticle stiffness (Vincent and Wegst, 2004; Li et al., 2020). Our findings showed that although the hind femur consists of a cuticle that is less sclerotized than those of the fore and mid femora, it can still reach a stiffness higher than that of the cuticle of the other two femora in the circumferential direction. This can be attributed to the different orientations of fibers in the cuticle of the hind femur, in comparison to the fore and mid femora; the orientation of the fibers around the circumference of the hind femur, as seen in Fig. 4e,f, leads to an increase of the elasticity modulus of the femur in this direction. Hence, our results suggest that both the microstructure and sclerotization of the cuticle sometimes enhance the influence of each other and sometimes may have opposing effects.

4.3. Functional significance of ridges in the hind femur

Hind femur is the only one among others that contains longitudinal ridges (Fig. 1a). The function of the ridges and why they appear only on the hind femur still remain matters of debate. Previous research has suggested that a potential function of similar ridges in different regions of insect exoskeleton is to enhance buckling resistance (Vincent and Wegst, 2004; Hecht and Cullinane, 2010). Although recent studies on the ridges of the hind tibiae of stick insects support this function (Schmitt et al., 2018; Xing and Yang, 2019), another research suggests otherwise (Parle et al., 2015). Under loading and before buckling takes place, the stress in the ridges can exceed the yield strength of the cuticle, so that the failure occurs as a result of plasticity (Parle et al., 2015). The latter finding, however, is based on the assumption

that cuticle is a homogeneous material. By contrast, as we have seen here, cuticle is inhomogeneous; both the microstructure and the sclerotization of the femur cuticle noticeably vary in different regions and, particularly, between the edges and the ridges.

Our findings suggest that the ridges can potentially enhance the total stiffness of the hind femur of the locust. This is based on two observations. First, the ridges are more sclerotized and, therefore, stiffer than other parts of the femur cuticle. Second, in contrast to the other regions with fibers that are all oriented circumferentially, they have extra layers in which fibers have a seemingly different orientation, i.e. along the length of the femur. As shown by the nanoindentation results, the two strategies have provided the ridges with a significantly higher stiffness than the edges (Fig. 5b). Our findings, therefore, support the conclusion made by Parle et al. (2015), who noted that the primary function of the ridges in the tibiae of stick insects is probably to increase the stiffness of the whole structure. Although, against our original hypothesis, the hind femur is generally less stiff than the fore and mid femora, the sclerotized ridges are likely to be stiff enough to enable the hind femur to withstand jumping stresses. However, it remains elusive why the increased stiffness has not been achieved by uniformly increasing the femur diameter that can perhaps provide a better solution with the same amount of material.

A previous study showed that a high level of sclerotization may have a serious consequence for insect cuticle: the increased risk of catastrophic failure. As an example, the highly sclerotized exoskeleton of the aposematic weevil *Pachyrhynchus sarcitis kotoensis*, would fail catastrophically when applied stresses exceed the strength of the cuticle (Wang et al., 2019). This may not cause a big challenge for the weevil body that should withstand occasional bites of lizard predators (Wang et al., 2018a). However, the risk of failure can be particularly high for the femur cuticle that is subjected to long-term cyclic stresses, increasing the likelihood of fatigue (Dirks et al., 2013). However, the fatigue failure of the hind femur might be prevented by the presence of the edges that have a relatively low sclerotization level. As we have seen here, the edges of the femur mainly consist of a non- or less-sclerotized cuticle and have an elasticity modulus that is significantly lower than that of the ridges. We suggest that, by providing the required flexibility, the cuticle of the ridges is able to absorb the energy that would otherwise lead to the failure of the femur material. This can explain why

the hind femur is generally less sclerotized than those of the fore and mid femora. A similar role has been suggested for the soft patches in prevention of dragonfly wing damage under frequent accidental collisions (Rajabi et al., 2020) and the soft cuticle at the buckling region of locust tibiae, which allow them to be used in jumping and defensive kicking without failure (Bayley et al., 2012). Future numerical/theoretical studies are needed to quantify the role of this design strategy on the durability of the femora, by measuring the energy absorbed by a real femur in a jumping cycle and comparing it with a femur that has uniform material properties similar to that of the ridges.

5. Conclusions

In this study, we attempted to establish a link between the microstructure, sclerotization, material properties and function of the femur cuticle of desert locusts. Based on our results, we can draw the following conclusions:

(i) The elasticity modulus of the hind femur, against our original hypothesis, is significantly lower than those of the fore and mid femora, in the longitudinal direction. This is likely to be a strategy to allow small deformations of the femur wall and reduce the risk of material failure.

(ii) Two strategies, i.e. stiff ridges in combination with relatively flexible edges, have come together to reach a compromise in the hind femur, making it compliant to prevent material failure, but stiff enough to withstand locomotion-related mechanical loads.

(iii) The sclerotized ridges of the hind femur increase the stiffness by increasing the elastic modulus of the femur cuticle.

(iv) Our results support the hypothesis that variations of the elasticity modulus in insect cuticle can largely be explained using interactions between the two key factors of microstructure and sclerotization.

Ethics

This work complies with ethical guidelines at Kiel University.

Competing interests

The authors declare there are no conflicts of interest to disclose.

Data accessibility

All supporting data are made available in the article.

Funding

This study was financially supported by "China Scholarship Council" to CL (Grant no. 201706400069).

Authors' contributions

Conceptualization: SNG and HR; Formal Analysis: CL; Funding Acquisition: CL and SNG; Investigation: CL; Methodology: CL, HR and SNG; Resources: SNG; Supervision: HR and SNG; Validation: CL; Visualization: CL; Writing – Original Draft Preparation: CL and HR; Writing – Review and Editing: CL, HR and SNG.

References

Andersen S O. Biochemistry of insect cuticle. Annual Review of Entomology, 1979, 24(1): 29-59.

Bayley T G, Sutton G P, Burrows M. A buckling region in locust hindlegs contains resilin and absorbs energy when jumping or kicking goes wrong. Journal of Experimental Biology, 2012, 215(7): 1151-1161.

Bennet-Clark H C. The energetics of the jump of the locust *Schistocerca gregaria*. Journal of Experimental Biology, 1975, 63(1): 53-83.

Caveney S. Muscle attachment related to cuticle architecture in Apterygota. Journal of Cell Science, 1969, 4(2): 541-559.

Dirks J H, Parle E, Taylor D. Fatigue of insect cuticle. Journal of Experimental Biology, 2013, 216(10): 1924-1927.

Eshghi S, Jafarpour M, Darvizeh A, Gorb, S N, and Rajabi H. A simple, high-resolution, non-destructive method for determining the spatial gradient of the elastic modulus of insect cuticle. Journal of the Royal Society Interface, 2018, 15(145): 20180312.

Gabriel J M. The development of the locust jumping mechanism: II. Energy storage and muscle mechanics. Journal of Experimental Biology, 1985, 118(1): 327-340.

Goodwyn P P, Peressadko A, Schwarz H, Kastner V and Gorb S. Material structure, stiffness, and adhesion: why attachment pads of the grasshopper (*Tettigonia viridissima*) adhere more strongly than those of the locust (*Locusta migratoria*) (Insecta: Orthoptera). Journal of Comparative Physiology A, 2006, 192(11): 1233-1243.

Hecht E M, Cullinane D M, Grosse I R. A novel stress distribution organ in the arthropod exoskeleton. Arthropod Structure and Development, 2010, 39(5): 305-309.

Heitler W J. The locust jump: III. Structural specializations of the metathoracic tibiae. Journal of Experimental Biology, 1977, 67(1): 29-36.

Hepburn H R, Chandler H D. Material properties of arthropod cuticles: the arthrodial membranes. Journal of Comparative Physiology A, 1976, 109(2): 177-198.

Hepburn H R, Joffe I. Locust solid cuticle - a time sequence of mechanical properties. Journal of Insect Physiology, 1974, 20(3): 497-506.

Hoyle G. The anatomy and innervation of locust skeletal muscle. Proceedings of the Royal

Society of London. Series B-Biological Sciences, 1955, 143(911): 281-292.

Li C, Gorb S N, Rajabi H. Cuticle sclerotization determines the difference between the elastic moduli of locust tibiae. Acta Biomaterialia, 2020, 103: 189-195.

Locke M, The structure and formation of the integument in insects. In: M. Rockstein (Ed.), The Physiology of Insecta, Academic Press, New York, 1974.

Matsumura Y, Jafarpour M, Ramm S A, Reinhold K, Gorb S N and Rajabi H. Material heterogeneity of male genitalia reduces genital damage in a bushcricket during sperm removal behaviour. The Science of Nature, 2020, 107(6): 1-10.

Matsumura Y, Kovalev A E, Gorb S N. Penetration mechanics of a beetle intromittent organ with bending stiffness gradient and a soft tip. Science Advances, 2017, 3(12): eaao5469.

Michels J, Appel E, Gorb S N. Functional diversity of resilin in Arthropoda. Beilstein Journal of Nanotechnology, 2016, 7(1): 1241-1259.

Michels J, Gorb S N. Detailed three‐dimensional visualization of resilin in the exoskeleton of arthropods using confocal laser scanning microscopy. Journal of Microscopy, 2012, 245(1): 1-16.

Müller M, Olek M, Giersig M and Schmitz H. Micromechanical properties of consecutive layers in specialized insect cuticle: the gula of *Pachnoda marginata* (Coleoptera, Scarabaeidae) and the infrared sensilla of *Melanophila acuminata* (Coleoptera, Buprestidae). Journal of Experimental Biology, 2008, 211(16): 2576-2583.

Neville AC. Biology of the Arthropod Cuticle. Springer-Verlag, Berlin, 1975.

Parle E, Herbaj S, Sheils F, Larmon H and Taylor D. Buckling failures in insect exoskeletons. Bioinspiration & Biomimetics, 2015, 11(1): 016003.

Parle E, Larmon H, Taylor D. Biomechanical factors in the adaptations of insect tibia cuticle. PloS One, 2016, 11(8): e0159262.

Peisker H, Michels J, Gorb S N. Evidence for a material gradient in the adhesive tarsal setae of the ladybird beetle *Coccinella septempunctata*. Nature Communications, 2013, 4(1): 1-7.

Rajabi H, Dirks J H, Gorb S N. Insect wing damage: causes, consequences and compensatory mechanisms. Journal of Experimental Biology, 2020, 223(9).

Rajabi H, Stamm K, Appel E and Gorb S N. Micro-morphological adaptations of the wing

nodus to flight behaviour in four dragonfly species from the family Libellulidae (Odonata: Anisoptera). Arthropod Structure and Development, 2018, 47(4): 442-448.

Richards A G. The cuticle of arthropods. Springer, Berlin, Heidelberg, 1958: 1-26.

Schmitt M, Büscher T H, Gorb S N and Rajabi H. How does a slender tibia resist buckling? Effect of material, structural and geometric characteristics on buckling behaviour of the hindleg tibia in stick insect postembryonic development. Journal of Experimental Biology, 2018, 221(4).

Scholz I, Baumgartner W, Federle W. Micromechanics of smooth adhesive organs in stick insects: pads are mechanically anisotropic and softer towards the adhesive surface. Journal of Comparative Physiology A, 2008, 194(4): 373-384.

Sun J, Tong J, Ma Y. Nanomechanical behaviours of cuticle of three kinds of beetle. Journal of Bionic Engineering, 2008, 5: 152-157.

Vincent J F V. Morphology and design of the extensible intersegmental membrane of the female migratory locust. Tissue and Cell, 1981, 13(4): 831-853.

Vincent, J. F. V. and Wegst, U. G. K. (2004). Design and mechanical properties of insect cuticle. Arthropod Structure and Development 33(3), 187-199.

Wan C, Hao Z, Feng X. Structures, properties, and energy-storage mechanisms of the semi-lunar process cuticles in locusts. Scientific Reports, 2016, 6(1): 1-13.

Wang L Y, Huang W S, Tang H C, Huang L C and Lin C P. Too hard to swallow: a secret secondary defence of an aposematic insect. Journal of Experimental Biology, 2018a, 221(2).

Wang L Y, Jafarpour M, Lin C P, Appel E, Gorb S N and Rajabi H. Endocuticle sclerotisation increases the mechanical stability of cuticle. Soft Matter, 2019, 15(41): 8272-8278.

Wang L Y, Rajabi H, Ghoroubi N, Lin C P and Gorb S N. Biomechanical strategies underlying the robust body armour of an aposematic weevil. Frontiers in Physiology, 2018b, 9: 1410.

Xing Y, Yang J. A Compromise reveals buckling resistance strategy of a naturally slender tibia. Advanced Theory and Simulations, 2019, 2(7): 1900051.

Figure captions:

Fig. 1. Specimens and measurement directions. (a) Natural postures and load directions of an adult locust. (b) 3D-reconstructions of fore, mid and hind femora. Three transverse sections along the length of each femur are shown. (c) Indentation directions (arrows): longitudinal, circumferential and radial directions. Scale bar: 1 mm. The colors in this panel are identical to those used in Figs. 2 and 3.

Fig. 2. Elasticity moduli of the femora in different directions. Elasticity moduli of the fore (n = 15), mid (n = 15), and hind femora (n = 15) are presented in the longitudinal, circumferential and radial directions. Detailed statistical comparisons are shown in Table 1.

Fig. 3. Sclerotization level of different femoral cuticles. Area fraction of the non-, less- and highly-sclerotized cuticle of the fore (n = 3), mid (n = 3) and hind femora (n = 3). Representative CLSM images in the right side panels show the transverse sections of the fore, mid and hind femora from the same locust (all from the right legs). Scale bars: 1 mm. FF: fore femur, MF: mid femur, HF: hind femur. ***: $P < 0.001$.

Fig. 4. Microstructure of the femoral cuticle. (a, b) SEM images of the transverse section (a) and the longitudinal section (b) of the fore femur showing the epi-, exo- and endocuticle. Majority of the fibers in the endocuticle are oriented along longitudinal axis in the fore femur. (c, d) SEM images of the transverse section (c) and the longitudinal section (d) of the mid femur showing the same fiber orientation as seen in the fore femur. (e, f) SEM images of the transverse section (e) and the longitudinal section (f) of the edges of the hind femur (see Fig.5a) show endocuticle fibers that are oriented along the circumference of the femur. epi: epitucicle, exo: exocuticle, endo: endocuticle.

Fig. 5. Elasticity modulus, sclerotization level and microstructure of the cuticle of ridges and edges of the hind femur. (a) Schematic drawing of the transverse section of the hind femur showing the ridges and edges. (b) Elasticity moduli of the ridges and edges in the longitudinal direction. (c, d) CLSM images of the ridges (c) and the edges (d). (e-g) SEM images of the ridges, showing the layered structure in the transverse section (e), and in the longitudinal section (f, g). (g) Magnified view of a unidirectional layer in the endocuticle of the ridge showing fibers that are oriented along the length of femur. epi: epicuticle, exo: exocuticle, endo: endocuticle. Scale bars: (c) 100 μm, (d) 50 μm, (e) 40 μm, (f) 40 μm, (g) 5 μm.

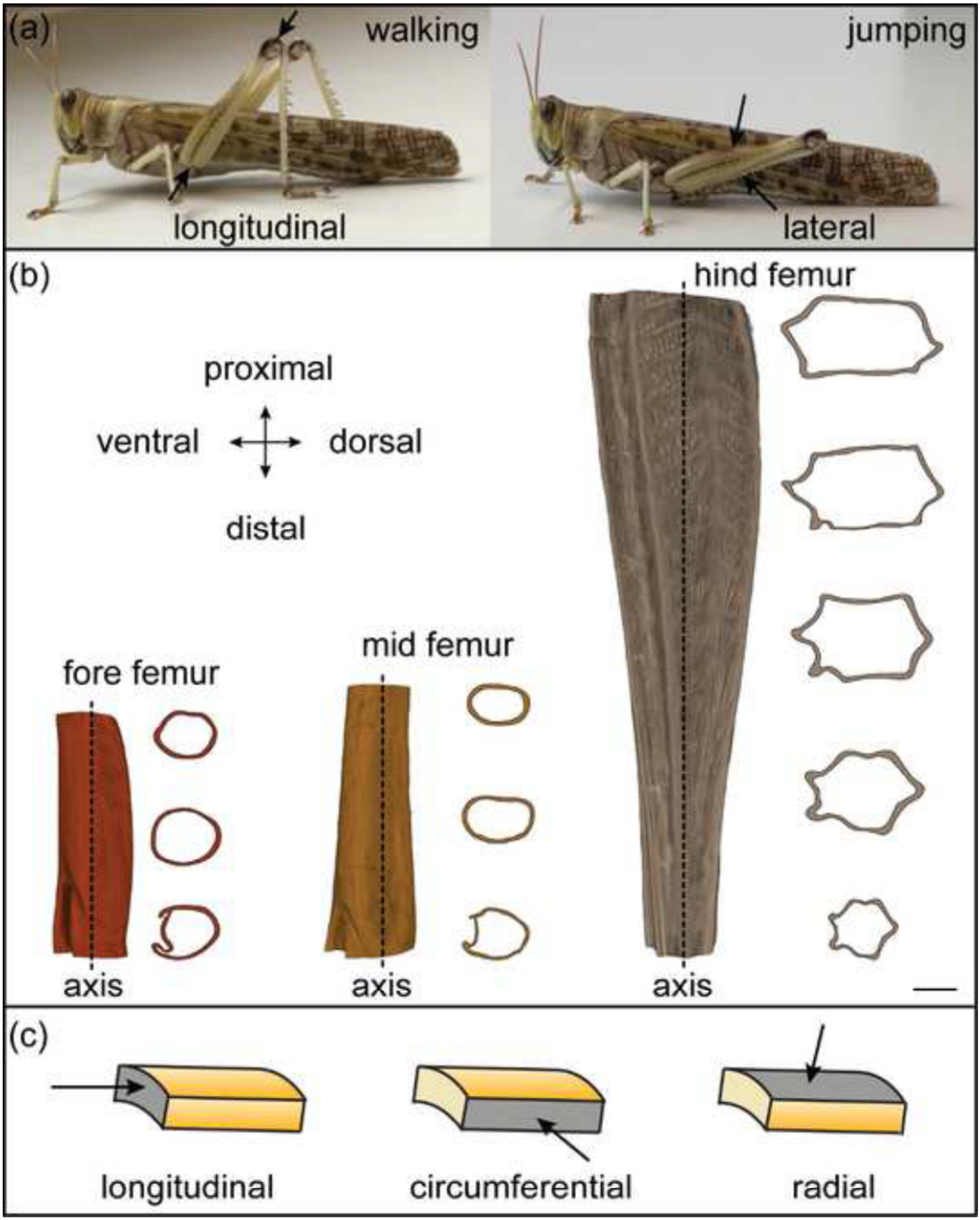

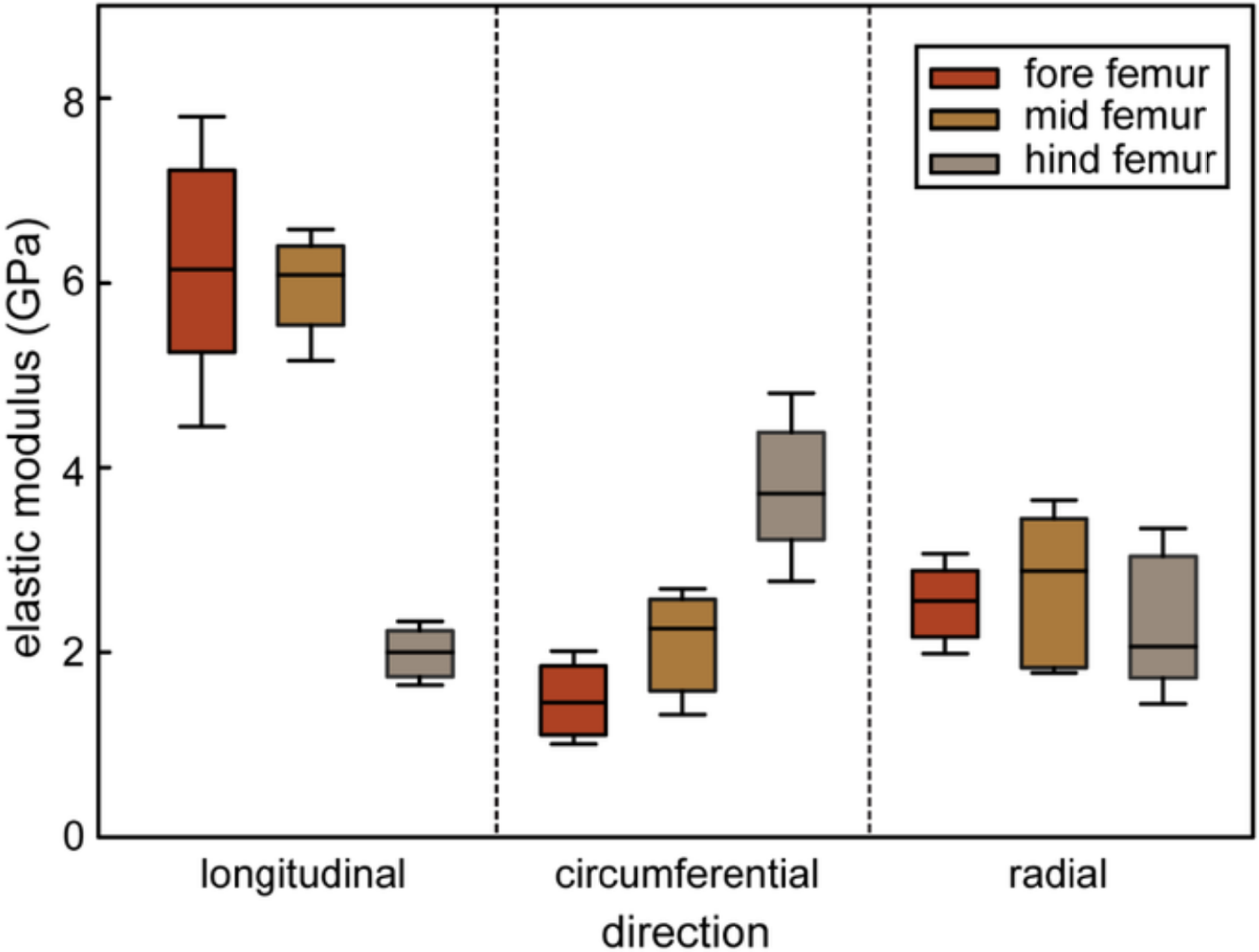

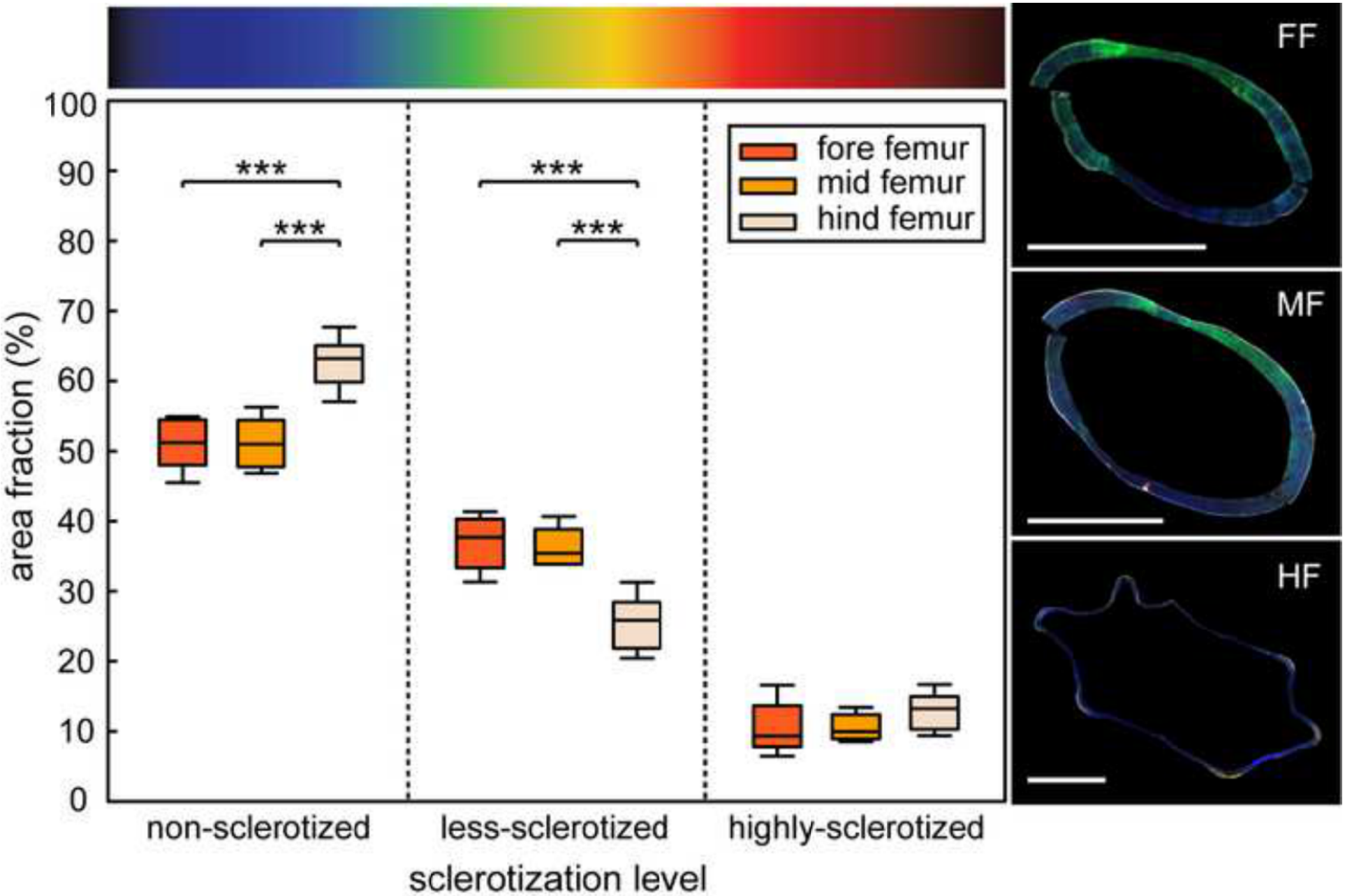

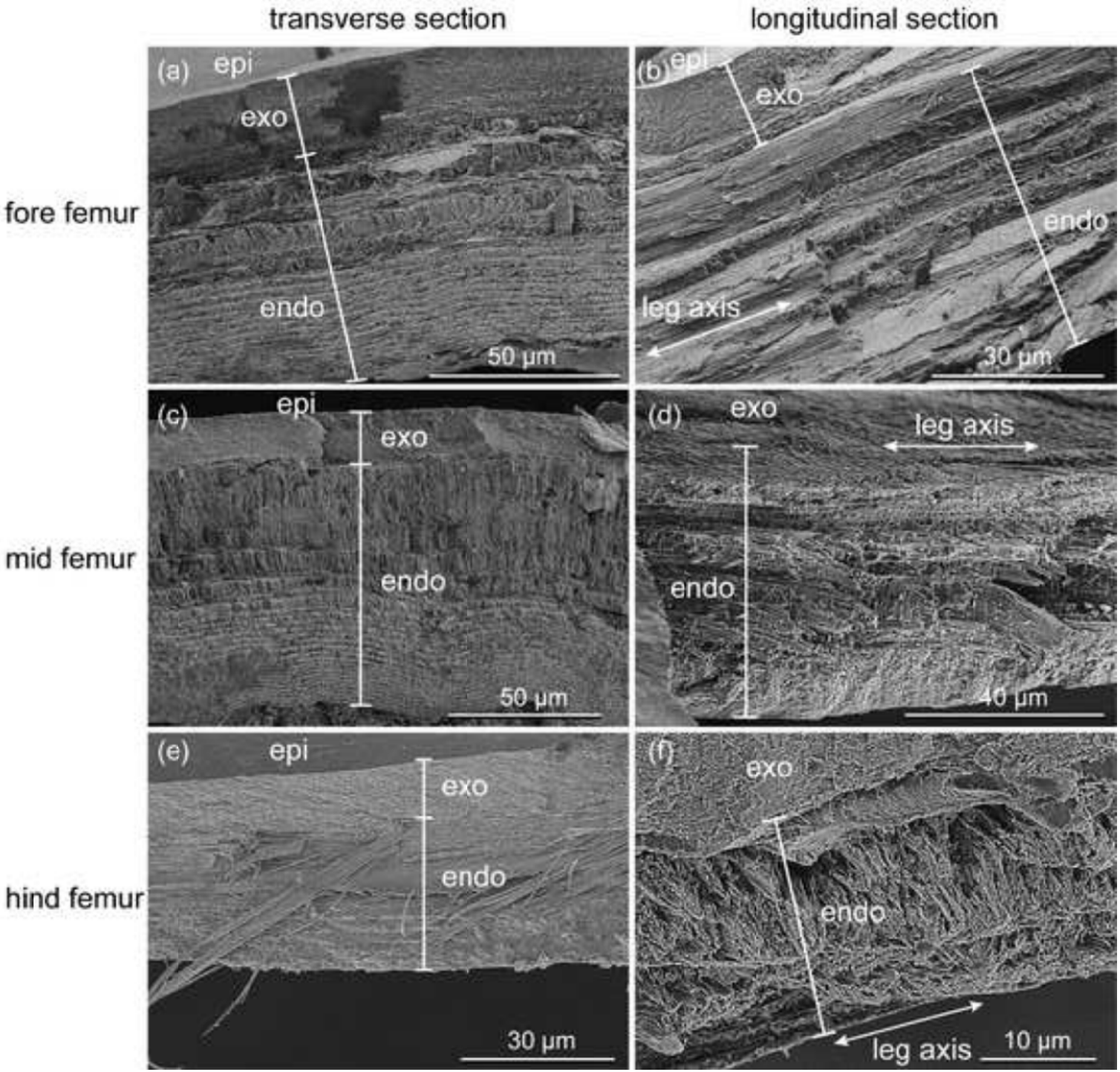

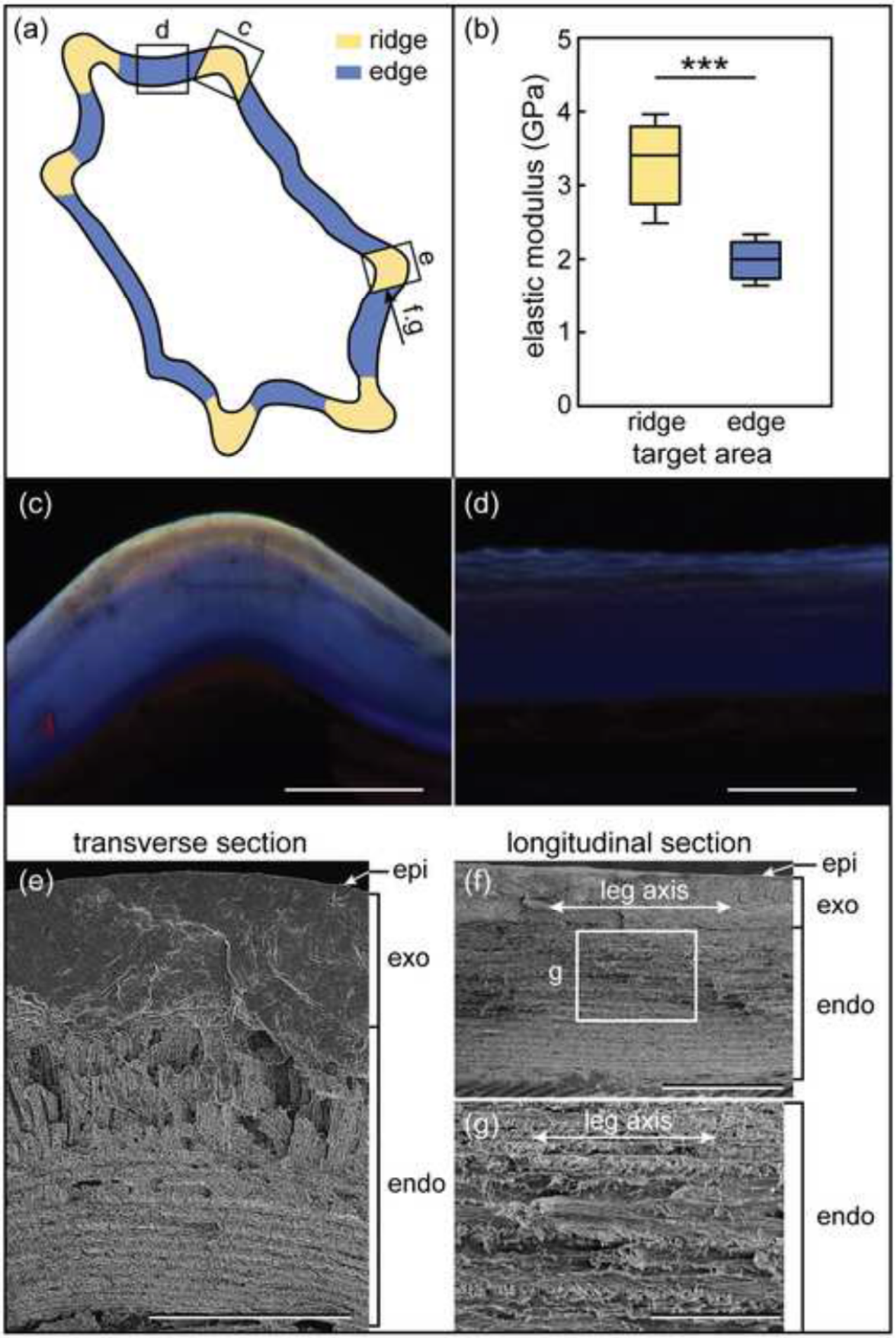
(a)
d
c
ridge
edge
e
f,g
(b)
***
elastic modulus (GPa)
0
1
2
3
4
5
ridge
edge
target area
(c)
(d)
transverse section
longitudinal section
(e)
epi
exo
endo
(f)
leg axis
g
epi
exo
endo
(g)
leg axis
endo

Declaration of interests

☒ The authors declare that they have no known competing financial interests or personal relationships that could have appeared to influence the work reported in this paper.

☐The authors declare the following financial interests/personal relationships which may be considered as potential competing interests: